Hindawi
Journal of Optimization
Volume 2018, Article ID 6258350, 19 pages
https://doi.org/10.1155/2018/6258350

Research Article

A Heuristic Approach for Optimal Planning and Operation of Distribution Systems

Khalid Mohammed Saffer Alzaidi[1,2] **Oguz Bayat,**[1] **and Osman N. Uçan**[1]

[1] *Engineering and Natural Sciences Facility, Altinbas University, Istanbul, Turkey*
[2] *Department of Computer Science, Faculty of Sciences, University of Diyala, Diyala, Iraq*

Correspondence should be addressed to Khalid Mohammed Saffer Alzaidi; kha2005ms@yahoo.com

Received 3 January 2018; Revised 14 April 2018; Accepted 29 April 2018; Published 3 June 2018

Academic Editor: Wei Wei

The efficient planning and operation of power distribution systems are becoming increasingly significant with the integration of renewable energy options into power distribution networks. Keeping voltage magnitudes within permissible ranges is vital; hence, control devices, such as tap changers, voltage regulators, and capacitors, are used in power distribution systems. This study presents an optimization model that is based on three heuristic approaches, namely, particle swarm optimization, imperialist competitive algorithm, and moth flame optimization, for solving the voltage deviation problem. Two different load profiles are used to test the three modified algorithms on IEEE 123- and IEEE 13-bus test systems. The proposed optimization model uses three different cases: Case 1, changing the tap positions of the regulators; Case 2, changing the capacitor sizes; and Case 3, integrating Cases 1 and 2 and changing the locations of the capacitors. The numerical results of the optimization model using the three heuristic algorithms are given for the two specified load profiles.

1. Introduction

Power systems have been evolving in the last two decades, exhibiting such changes as deregulation and the integration of renewables into the philosophical and operational mentalities. From the operational point of view, control means that involving the coordinated operation of tap changing transformers, such as capacitors, is required because loads are not constant over time and the outputs of renewable energy sources are intermittent. Voltage optimization (VO) is an effective technology that has been saving the industry millions of dollars in wasted electrical energy since the beginning of the new millennium [1]. High demand used to be managed by voltage reduction [2]. Another way of helping system operation is using capacitors to improve the power factor and the voltage profile and reduce power losses [3]. Furthermore, tap operations of voltage regulators are helpful in enhancing voltage profiles. Capacitors and voltage regulators are integrated, and improved voltage profiles are obtained. However, the life span of these devices is shortened by frequent operation because they are based on mechanical switch operations. New technological developments have made electronics-based voltage regulators and capacitors available [4], thereby bringing additional flexibility into the operation of smart grids.

On the planning side, optimal capacitor locations are sought [4]. For instance, in an algorithm that depends on dynamic programming, fuzzy logic and genetic algorithm (GA) approaches are used for capacitor distribution in distribution feeders. Gravitational search algorithm was used for optimal capacitor placement in [5], whereas a teaching-learning-based optimization was used for the same aim in [6]. Capacitors can also be used to reduce the effects of harmonics in distribution systems; the harmony search algorithm was applied for this goal in [7]. Capacitor location and sizing problem have been solved by other heuristics, such as clonal selection algorithm [8], ant colony optimization algorithm [8], and PSO [9].

Producing the best possible result with the available resources is always an objective in engineering problems. Optimization problems are generally solved using two approaches. The first is based on mathematical analysis, and the second is based on numerical calculations. Numerical optimization methods can be divided into derivative-based and non-derivative-based methods. If the derivatives of the encountered model are not easy to find or a mathematical function related to the model does not exist, then non-derivative-based methods are applied. These methods are generally inspired by nature. The most popular model is GA, which reflects the evolution process in nature [10]. Subsequently, methods inspired by the behaviors of birds and fish (particle swarm optimization [PSO]) [11], improvisation process of musicians (harmony search) [12], and the navigation approach of moths in nature, which is named transverse orientation (moth flame optimization [MFO]) [13], were developed.

This work models the voltage optimization problem using three different heuristic algorithms, namely, imperialist competitive algorithm (ICA), particle swarm optimization (PSO), and moth flame optimization (MFO). Cases 1 and 2 are applicable to operation, and Case 3 is applicable to planning in distribution systems.

(i) The first model changes and uses the tap positions of the voltage regulators and obtains the optimal voltage value for given load conditions of the distribution system.

(ii) The second model uses only the capacitors and optimizes the sizes of these devices for given load conditions.

(iii) The third model uses the voltage regulators and the capacitors and finds the optimal tap positions, capacitor sizes, and locations.

MATLAB and a free power distribution system simulation tool OpenDSS [14, 15] are used in the simulations.

The rest of the paper is organized as follows. Section 2 proposes the voltage optimization models. Section 3 briefly explains ICA, PSO, MFO, and modified algorithm-based voltage deviation. Section 4 presents the experiments and the simulation results. Section 5 presents the conclusions.

2. Model

We model three different cases.

Case 1. This case considers tap changers for the voltage regulators to minimize voltage deviations. The optimization model is as follows:

$$\text{Minimize} \quad (x) = \sum_{i=1}^{N} \left\| V_i - 1 \right\|^2, \quad V_i = f\left(\text{Tap}_i\right) \tag{1}$$

$$\text{Subject to:} \quad 0.95 \le V_i \le 1.05 \tag{2}$$

$$\text{Tap}_{\min} \le \text{Tap}_i \le \text{Tap}_{\max}, \tag{3}$$

where x denotes the fitness values (cost), N is the number of buses, V_i is the voltage magnitude of bus i, Tap_i is the tap position of the regulator, and $\text{Tap}_{\min}$ and $\text{Tap}_{\max}$ represent the minimum and maximum positions that a tap in a regulator can take, respectively. These values are in the range of $[-16, 16]$.

Case 2. This case considers changing the size of the capacitors, and the model is as follows:

$$\text{Minimize} \quad (x) = \sum_{i=1}^{N} \left\| V_i - 1 \right\|^2, \quad V_i = f\left(\text{Cap}_i\right) \tag{4}$$

$$\begin{aligned} \text{Subject to:} \quad & 0.95 \le V_i \le 1.05 \\ & 0 \le \text{Cap}_i \le \text{Cap}_{\max}, \end{aligned} \tag{5}$$

where x represents the fitness values (cost), N is the number of buses, V_i is the voltage magnitude of bus i, Cap_i is the size of the bank capacitor, and $\text{Cap}_{\max}$ is the maximum size of the bank capacitor.

Case 3. This case integrates Cases 1 and 2 and changes the locations of the capacitors. The mathematical model is as follows:

$$\begin{aligned} \text{Minimize} \quad & (x) = \sum_{i=1}^{N} \left\| V_i - 1 \right\|^2, \\ & V_i = f\left(\text{Tap}_i, \text{Cap}_i, l_i\right) \end{aligned} \tag{6}$$

$$\begin{aligned} \text{Subject to:} \quad & 0.95 \le V_i \le 1.05 \\ & \text{Tap}_{\min} \le \text{Tap}_i \le \text{Tap}_{\max} \\ & 0 \le \text{Cap}_i \le \text{Cap}_{\max} \\ & 2 \le l_i \le L_{\max}, \end{aligned} \tag{7}$$

where x represents the fitness values (cost), N is the number of buses, V_i is the voltage magnitude of bus i, Tap_i is the tap position of the regulator, $\text{Tap}_{\min}$ and $\text{Tap}_{\max}$ represent the minimum and maximum positions that a tap in a regulator can take, respectively (these values are in the range of $[-16, 16]$), Cap_i is the size of the bank capacitor, $\text{Cap}_{\max}$ is the maximum size of the bank capacitor, l_i represents the location of the capacitors, and $L_{\max}$ represents the maximum bus location.

3. Heuristic Algorithms

3.1. Imperialist Competitive Algorithm (ICA)

3.1.1. General Approach. ICA was recently developed in 2007 by Esmaeil Gargari and Caro Lucas for continuous optimization problems [16]. The working philosophy corresponds to other evolutionary algorithms and initially creates random solution candidates called countries. The cost function of each solution candidate shows the power of each country. Hence, populations are composed of either colonized or imperialist countries. According to random rules, a part of a population is selected as the imperialists or the powerful countries, and the remaining part of the population comprises the colonized. Figure 1 presents a flowchart of ICA [16].

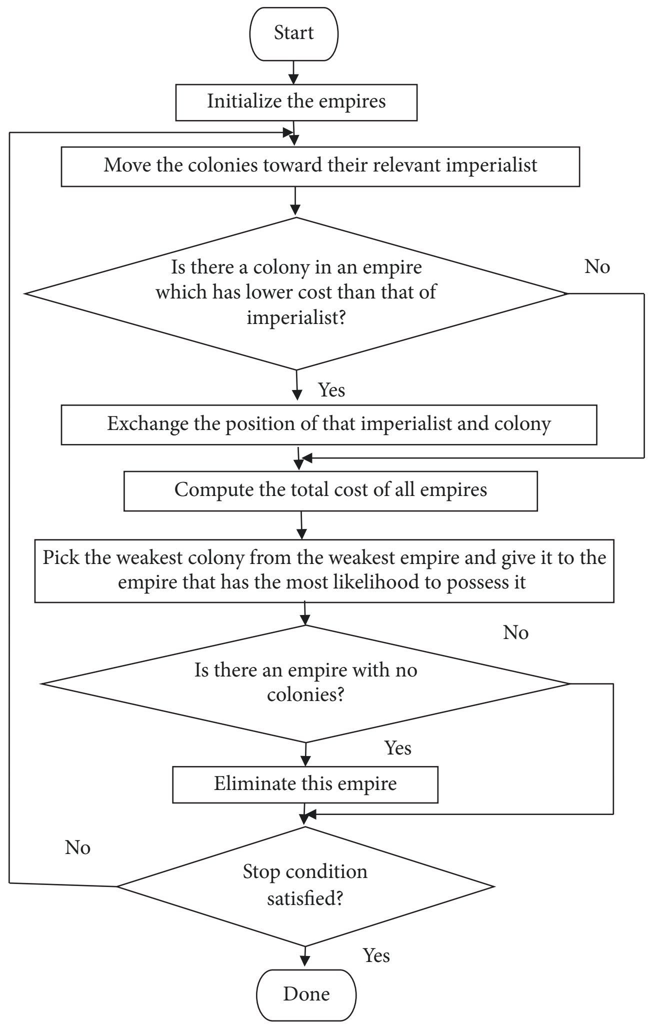

Figure 1: Flowchart of ICA [16].

The method is conducted as follows:

(i) Form countries: the ith country is formed as follows:

$$\text{country}_i = [P_1, P_2, P_3, \ldots, P_{\text{DN}}], \quad (8)$$

where DN denotes the problem variables or dimensions. Initial random values for P_i should be within the lower and upper ranges for each variable.

(ii) Find the powers of each country by evaluating the objective function of the optimization problem as follows:

$$f(\text{country}_i) = f(P_1, P_2, P_3, \ldots, P_{\text{DN}}) \quad (9)$$

(iii) Select the imperialist and colonized countries. The power of a country is inversely symmetrical to its cost. The division of colonies among imperialists and the normalized value of each imperialist is defined as follows:

$$C_n = c_n - \max(c_i), \quad (10)$$

where c_n is the cost of nth imperialist and C_n is the normalized value.

(iv) Then, the colony countries move to the imperialist ones to start the optimization process. The DN country population is generated, and N_{imp} represents the most powerful population, whose members are selected as imperialists (the sets of controller coefficients with smaller cost function in this problem). The remaining N_{col} countries are the colonies (the sets of controller coefficients with a high cost function in this problem), each of which is a part of one of the above-mentioned empires. In the attraction policy, the colonies move toward the imperialists along Mx units and are situated in a new position. Mx is a random variable with regular distribution and can be expressed as follows:

$$\text{Mx} \sim U(0, \beta \cdot ds), \quad (11)$$

where β is a constant number greater than 1 ($\beta = 2$) and ds is the space between imperialist and colony. To

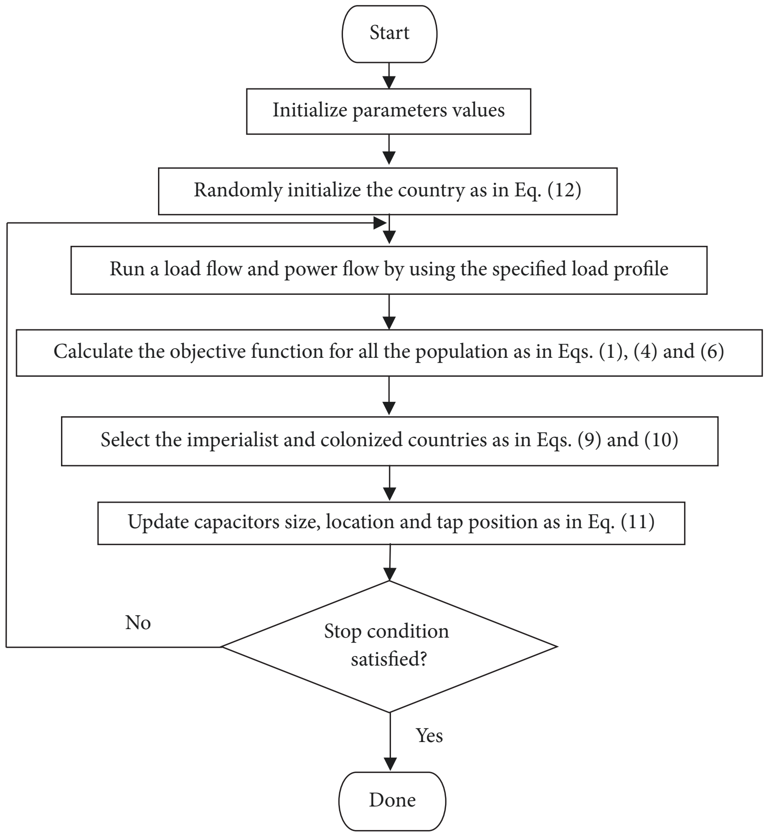

Figure 2: Flowchart of modified ICA.

search different points around the imperialist, we add a random amount θ of deviation to the direction of movement as follows:

$\theta \sim U(-\Upsilon, \Upsilon)$, where Υ is a parameter to adjust the deviation value ($\Upsilon = \pi/4$).

(v) Calculate total power of an empire. It can be determined by the power of imperialist country plus percentage of power of its colonies as follows:

T.C.n = cost (imperialist) + Ƹ$\cdot$ mean (cost (colonies of empire)), where T.C.n is the total cost of nth empire and Ƹ is a positive number that is considered to be less than 1 (Ƹ $= 0.02$). The weakest colony of the weakest empire is picked out.

There are some other hyperparameters used in the internal calculations of this algorithm; for example, the percent of search space size is a positive number (0.02), which enables the uniting process of two empires, α is a number in the interval of $[0 \ \ 1]$ and denotes the importance of mean minimum compares to the global minimum, and revolution rate is a positive number (0.3) representing the process in which the sociopolitical characteristics of a country change suddenly.

3.1.2. ICA-Based Voltage Deviation Algorithm. The flowchart of the modified ICA algorithms is shown in Figure 2, and the steps are as follows.

Step 1. Initialize the ICA parameters, namely, population size N_{pop}, maximum iteration number Max_{it}, number of imperialist countries N_{imp}, and number of colony countries N_{col}. Set the voltage magnitude limits, and set the possible capacitor locations, capacitor size limits, and minimum and maximum tap positions depending on the case being solved.

Step 2. Randomly create the size and location of the capacitors and tap positions of the regulators, and form the initial country as follows:

$$\text{country}_i = [\text{Cap}_1, \ldots, \text{Cap}_m, l_1, \ldots, l_m, \text{Tap}_1, \ldots, \text{Tap}_n], \qquad (12)$$

where m and n represent the numbers of bank capacitors and voltage regulators, respectively.

Step 3. Run a load flow using the specified load profile and the solution candidates, perform a power flow, and calculate the fitness value of the test system depending on the case number as in (1), (4), and (6).

Step 4. Determine the imperialist and colonized countries depending on the fitness value as in (9) and (10).

Step 5. Update the size and location of the capacitors and the tap position of the regulators for all empires as in (11).

Step 6. Repeat Steps 3–5 until the stopping condition is met.

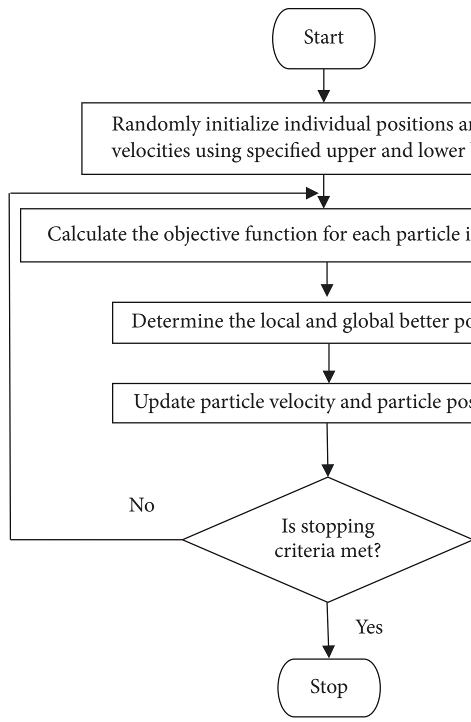

Figure 3: Flowchart of PSO algorithm.

3.2. Particle Swarm Optimization (PSO)

3.2.1. General Approach. PSO was originally developed in 1995 by Kennedy and Eberhart and inspired by the social behavior of schooling fish and flocking birds [17]. The birds in a group are considered an individual in the PSO method. These particles can be flown through a search space. The location of a particle in the search problem represents one solution for the problem. A new and different solution is created when the individual moves to a new location in the search space. Each solution can be evaluated using an objective function that supplies a cost of the benefit of the solution. The direction and velocity of each individual can move along all dimensions of the search space and thus can change with all generation of movement. PSO is generally considered an evolutionary computation (EC) sample. Other EC examples include evolutionary strategies, genetic programming, evolutionary programming, and GA [18]. Each individual i maintains the following information [19]:

(i) X_i is the individual current position.

(ii) V_i is the individual current velocity.

(iii) Y_i is the local better position of the individual (pbest), the better position visited yet by the individual.

(iv) $\hat{Y}$ is the global better position of the swarm (gbest), the better position visited yet by the entire swarm.

Figure 3 shows a flowchart of the PSO algorithm.

By using the above notation, the method is implemented as follows:

(1) Initialize the set constants, such as swarm size, dimension of the problem, maximum number of iterations, and upper and lower bounds.

(2) Randomly initialize the individual positions.

(3) Randomly initialize the individual velocities.

(4) Repeat until the stopping condition is met.

(5) Evaluate the fitness values using the objective function.

(6) Determine pbest and gbest.

(7) Determine the alteration particle velocity vector as follows:

$$V_i(t+1) = W \cdot V_i(t) + c_1 \cdot r_1(t) \cdot \left(Y_i(t) - X_i(t)\right) + c_2 \cdot r_2(t) \cdot \left(\hat{Y}(t) - X_i(t)\right), \quad (13)$$

where, t represents current iteration, $r_1(t)$ and $r_2(t)$ represent uniform random numbers between 0 and 1, acceleration coefficients are $c1$ and $c2$, usually between 0 and 4, and W represents the inertia weight; a damping factor, usually decreasing from around 0.9 to around 0.4 during the computation, is calculated as follows:

$$W = \frac{(\text{Max}_{\text{it}} - t)}{\text{Max}_{\text{it}}}, \quad (14)$$

where maximum number of iterations is Max_{it}.

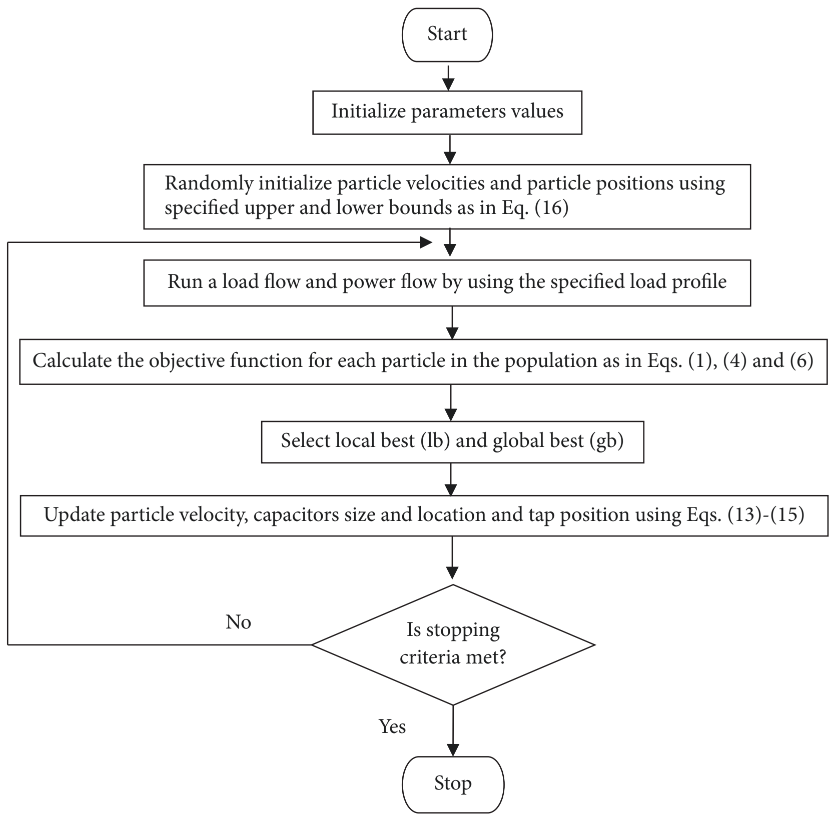

Figure 4: Flowchart of modified PSO algorithm.

(8) Determine the alteration particle position vector as follows:

$$X_i(t+1) = X_i(t) + V_i(t+1). \tag{15}$$

3.2.2. PSO-Based Voltage Deviation Algorithm. A flowchart of the modified PSO algorithms is shown in Figure 4, and the steps are as follows.

Step 7. Initialize the PSO parameters, namely, swarm size P_{size}, dimension of the problem N_{par}, maximum number of iterations Max_{it}, cognitive parameter c_1, social parameter c_2, upper bound value ub, lower bound value lb, and maximum velocity value $V_{\max}$. Set the voltage magnitude limits, and set the possible capacitor locations, capacitor size limits, and minimum and maximum tap positions depending on the case being solved.

Step 8. Randomly create the initialized particle velocities, determine the size and location of the capacitors and tap positions of the regulators, and form particle positions as follows:

$$\text{particle}_i = [\text{Cap}_1, \ldots, \text{Cap}_m, l_1, \ldots, l_m, \text{Tap}_1, \ldots, \text{Tap}_n], \tag{16}$$

where m and n represent the numbers of bank capacitors and voltage regulators, respectively.

Step 9. Run a load flow using the specified load profile, perform power flow using the solution candidates, and compute the corresponding fitness value of the test system depending on the case number as in (1), (4), and (6).

Step 10. Select local best (lb) and global best (gb), and then determine alteration particle velocity vector and particle positions as in (13)–(15).

Step 11. Repeat Steps 3 and 4 until the stopping condition is met.

3.3. Moth Flame Optimization (MFO)

3.3.1. General Approach. MFO is a new population-based algorithm refined in 2015 by Mirjalili; the optimization of this algorithm reflects transverse orientation, which is the method of transmission of moths in nature at night [13]. Approximately 160,000 different groups of insects, including moths, are present in nature. Moths have two life phases: larvae and adult phases. These insects are considerably similar to the family of butterflies but possess a special feature when moving at night [20]. Moths fly straight lines over long distances by preserving a fixed angle with the moon. This mechanism is effective for traveling, especially when the light source is far. When the light source is close, moths fly around it in a spiral path and ultimately converge with it. These insects represent the candidate solutions, and their position in the search space represents the problem variables.

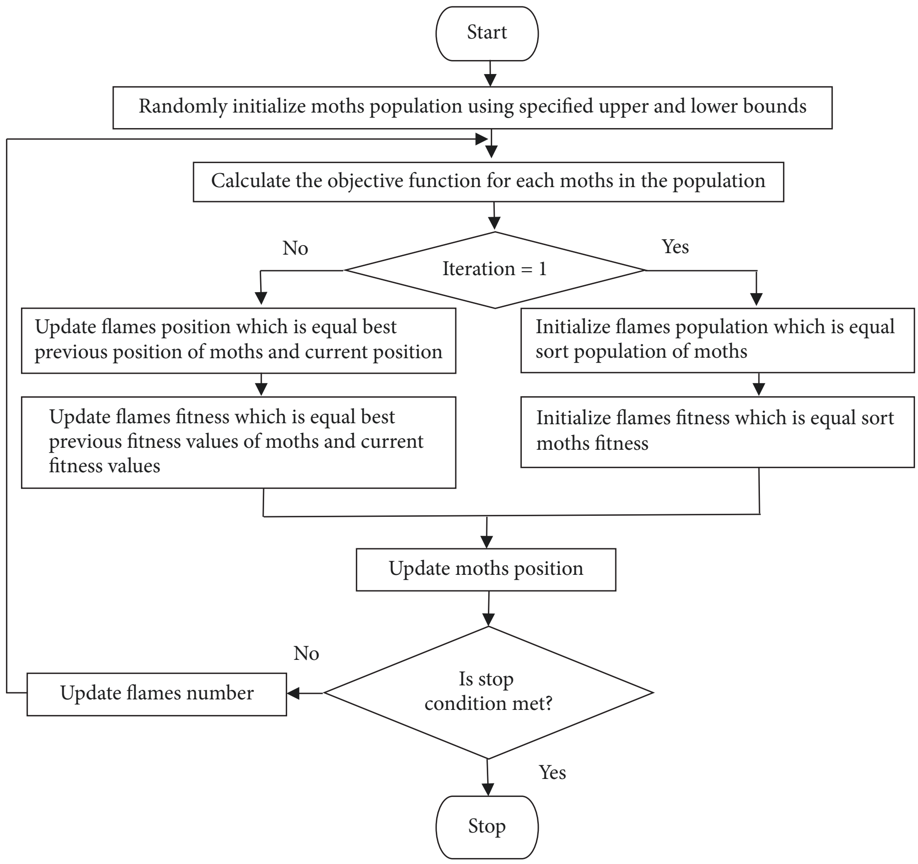

Figure 5: Flowchart of MFO algorithm.

Therefore, moths can fly in one or more dimensions by updating the position vectors. Figure 5 presents a flowchart of the MFO algorithm.

This model is implemented as follows:

(1) Initialize the set constants, such as number of moths, number of variables (dimension), and upper and lower bounds.

(2) Randomly initialize the population of moths depending on the number of moths, number of variables, and upper and lower bounds as follows:

$$\mathbf{Mo} = \begin{bmatrix} \mathrm{Mo}_{11} & \cdots & \mathrm{Mo}_{1d} \\ \mathrm{Mo}_{21} & \cdots & \mathrm{Mo}_{2d} \\ \vdots & \ddots & \vdots \\ \mathrm{Mo}_{n1} & \cdots & \mathrm{Mo}_{nd} \end{bmatrix}, \quad (17)$$

where n and d represent the numbers of moths and variables, respectively.

(3) Calculate and store the corresponding fitness values for all the moths as follows:

$$\mathbf{OMo} = \begin{bmatrix} \mathrm{OMo}_1 \\ \mathrm{OMo}_2 \\ \vdots \\ \mathrm{OMo}_n \end{bmatrix}, \quad (18)$$

where n represents the number of moths.

(4) Initialize the population of flames, which is equal sort population of moths, and flame fitness values, which are the equal sort moth fitness values.

$$\mathbf{F} = \begin{bmatrix} F_{11} & \cdots & F_{1d} \\ F_{21} & \cdots & F_{2d} \\ \vdots & \ddots & \vdots \\ F_{n1} & \cdots & F_{nd} \end{bmatrix}, \quad (19)$$

$$\mathbf{OF} = \begin{bmatrix} \mathrm{OF}_1 \\ \mathrm{OF}_2 \\ \vdots \\ \mathrm{OF}_n \end{bmatrix}, \quad (20)$$

where n and d represent the numbers of moths and variables, respectively.

Table 1: Active and reactive loads on IEEE 13-bus for simulation I (minimum load) and simulation II (maximum load).

Bus number	Phases	Active load of simulation I (kW)	Active load of simulation II (kW)	Reactive load (kVar)	Load type
671	a, b, c	854	1153	660	Delta
634	a	98	160	110	Wye
634	b	79	120	90	Wye
634	c	80	120	90	Wye
645	b	106	170	125	Wye
646	b, c	160	230	132	Delta
692	a, b, c	102	170	151	Delta
675	a	320	485	190	Wye
675	b	44	68	60	Wye
675	c	202	290	212	Wye
611	c	111	169	80	Wye
652	a	80	128	86	Wye
670	a	11	17	10	Wye
670	b	42	66	38	Wye
670	c	75	117	68	Wye

(5) Repeat until the stopping condition is met.

(6) Calculate the distance between the jth flame and the ith moth as follows:

$$D_i = \left|F_j - \mathrm{Mo}_i\right|. \tag{21}$$

(7) Update the position of moths using a spiral function as follows:

$$\mathrm{Mo}_i = D_i \cdot e^{bt} \cdot \cos(2\pi t) + F_j, \tag{22}$$

where D_i represents the distance, t is a random value in $[-1, 1]$, and b is a constant number.

(8) Update the flame position, which is equal to the best previous moth position and the current moth position (same as flame fitness values) as follows:

$$F = \mathrm{Sort}\left(\mathrm{Mo}_{i-1}, \mathrm{Mo}_i\right) \tag{23}$$

$$\mathrm{OF} = \mathrm{Sort}\left(\mathrm{OMo}_{i-1}, \mathrm{OMo}_i\right), \tag{24}$$

where i represents the current iteration.

3.3.2. MFO-Based Voltage Deviation Algorithm. A flowchart of the modified MFO algorithms is shown in Figure 6, and the steps are as follows.

Step 12. Initialize the MFO parameters, namely, the number of moths N, variable number D, maximum number of repetitions $\mathrm{Max}_{\mathrm{it}}$, upper bound value ub, and lower bound value lb. Set the voltage magnitude limits, and set the possible capacitor locations, capacitor size limits, and minimum and maximum tap positions depending on the case being solved.

Step 13. Randomly create the size and location of the capacitors and tap positions of the regulators, and form the initial moth position as in (17).

Step 14. Use the specified load profile to run a load flow, perform power flow using the solution candidates, and calculate the moth fitness value of the test system as in (18). Use (1), (4), and (6) depending on the case number.

Step 15. Select the best moth position as a flame position and the best moth fitness value as the flame fitness value using (23) and (24), as shown in (19) and (20), respectively.

Step 16. Calculate the distance between moths and flames, and then calculate new moth position using (21) and (22).

Step 17. Repeat Steps 3–5 until the stopping condition is met.

4. Experiments and Simulation Results

The proposed optimization models are experimented on IEEE 13- and IEEE 123-bus test systems. The node maps of the circuits are shown in Figures 7 and 8, respectively.

The different load conditions are given in Tables 1 and 2 and are denoted as simulation I (minimum load) and simulation II (maximum load) on the IEEE 13- and IEEE 123-bus test systems, respectively.

Graphical representations of the bus voltage magnitudes in pu of simulations I and II with no control (test systems do not contain tap regulators and capacitor banks) are shown in Figures 9 and 10 for the IEEE 13- and IEEE 123-bus test systems, respectively. The minimum and maximum voltage magnitudes in pu with no control of IEEE 13-bus test system in simulation I are 0.9081 and 0.99995, respectively, and in simulation II they are 0.89236 and 0.99993, respectively.

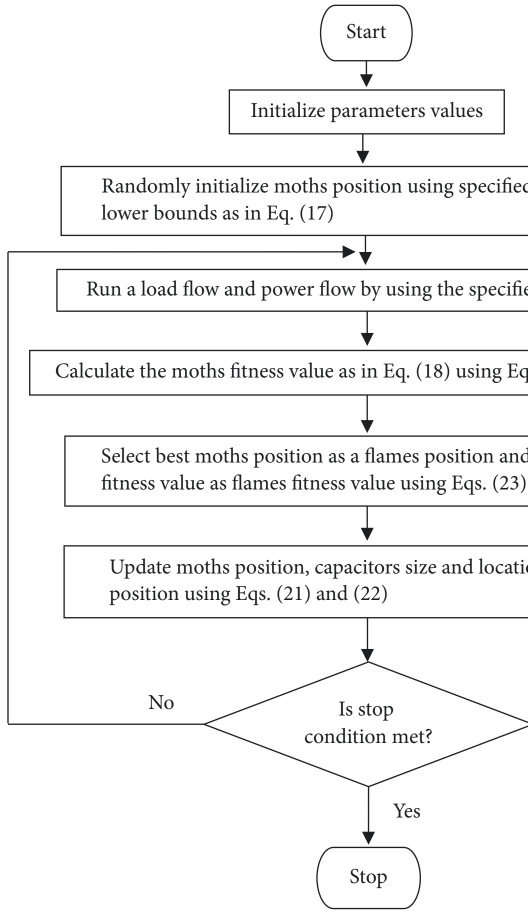

Figure 6: Flowchart of modified MFO algorithm.

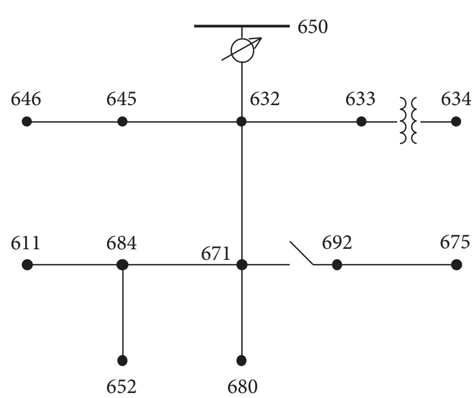

Figure 7: IEEE 13-bus node map.

The minimum and maximum voltage magnitudes in pu with no control of IEEE 123-bus test system in simulation I are 0.93317 and 0.99999, respectively, and in simulation II they are 0.91934 and 0.99999, respectively. The optimization model results for all cases, which are based on modified heuristic approaches ICA, PSO, and MFO, are graphically compared to uncontrolled results, as shown in Figures 11–16 for the IEEE 13- and IEEE 123-bus test systems, respectively.

The numerical results in Tables 3 and 4 support graphically results in Figures 11–16, respectively.

The smooth curves in Figures 11–16 represent the performance of Cases 1–3. Good voltage profile is observed in Case 3, in which tap regulator position and capacitor size and location are controlled. Through the curves in Figures 11–16, the voltage magnitudes can be obtained within the admissible range in any of the cases. The comparison of the simulation results that are based on ICA, PSO, and MFO is given in Figures 17–19. The numerical results in Tables 3–6 support graphically results in Figures 17–19.

Table 2: Active and reactive loads on IEEE 123-bus for simulation I (minimum load) and simulation II (maximum load).

Bus number	Phases	Active load of simulation I (kw)	Active load of simulation II (kw)	Reactive load (kVar)	Load type	Bus number	Phases	Active load of simulation I (kw)	Active load of simulation II (kw)	Reactive load (kVar)	Load type
1	a	30	37	20	Wye	62	c	25	39	20	Wye
2	b	12	19	10	Wye	63	a	27	39	20	Wye
4	c	26	38	20	Wye	64	b	50	75	35	Wye
5	c	13	19	10	Wye	65	a	23	35	25	Delta
6	c	25	38	20	Wye	65	b	24	35	25	Delta
7	a	14	19	10	Wye	65	c	52	69	50	Delta
9	a	24	38	20	Wye	66	c	52	72	35	Wye
10	a	13	20	10	Wye	68	a	12	20	10	Wye
11	a	26	40	20	Wye	69	a	25	40	20	Wye
12	b	14	20	10	Wye	70	a	13	20	10	Wye
16	c	26	39	20	Wye	71	a	26	40	20	Wye
17	c	12	20	10	Wye	73	c	27	40	20	Wye
19	a	26	38	20	Wye	74	c	28	40	20	Wye
20	a	26	39	20	Wye	75	c	28	38	20	Wye
22	b	25	39	20	Wye	76	a	62	104	80	Delta
24	c	26	40	20	Wye	76	b	46	70	50	Delta
28	a	28	40	20	Wye	76	c	45	70	50	Delta
29	a	28	39	20	Wye	77	b	26	40	20	Wye
30	c	24	39	20	Wye	79	a	27	40	20	Wye
31	c	13	20	10	Wye	80	b	30	40	20	Wye
32	c	14	20	10	Wye	82	a	29	38	20	Wye
33	a	26	40	20	Wye	83	c	12	20	10	Wye
34	c	25	40	20	Wye	84	c	13	19	10	Wye
35	a	28	40	20	Delta	85	c	25	40	20	Wye
37	a	28	39	20	Wye	86	b	13	20	10	Wye
38	b	12	19	10	Wye	87	b	27	40	20	Wye

Table 2: Continued.

Bus number	Phases	Active load of simulation I (kw)	Active load of simulation II (kw)	Reactive load (kVar)	Load type	Bus number	Phases	Active load of simulation I (kw)	Active load of simulation II (kw)	Reactive load (kVar)	Load type
39	b	13	20	10	Wye	88	a	29	40	20	Wye
41	c	12	19	10	Wye	90	b	29	39	20	Wye
42	a	13	20	10	Wye	92	c	24	40	20	Wye
43	b	25	40	20	Wye	94	a	26	40	20	Wye
45	a	15	19	10	Wye	95	b	14	20	10	Wye
46	a	14	19	10	Wye	96	b	13	20	10	Wye
47	a, b, c	64	103	75	Wye	98	a	26	40	20	Wye
48	a, b, c	137	202	150	Wye	99	b	30	40	20	Wye
49	a	23	35	25	Wye	100	c	28	39	20	Wye
49	b	45	69	50	Wye	102	c	12	20	10	Wye
49	c	23	35	20	Wye	103	c	27	39	20	Wye
50	c	29	39	20	Wye	104	c	26	39	20	Wye
51	a	15	19	10	Wye	106	b	25	40	20	Wye
52	a	25	40	20	Wye	107	b	25	40	20	Wye
53	a	26	40	20	Wye	109	a	29	40	20	Wye
55	a	13	20	10	Wye	111	a	15	20	10	Wye
56	b	13	20	10	Wye	112	a	11	20	10	Wye
58	b	13	20	10	Wye	113	a	25	40	20	Wye
59	b	15	19	10	Wye	114	a	13	20	10	Wye
60	a	14	19	10	Wye						

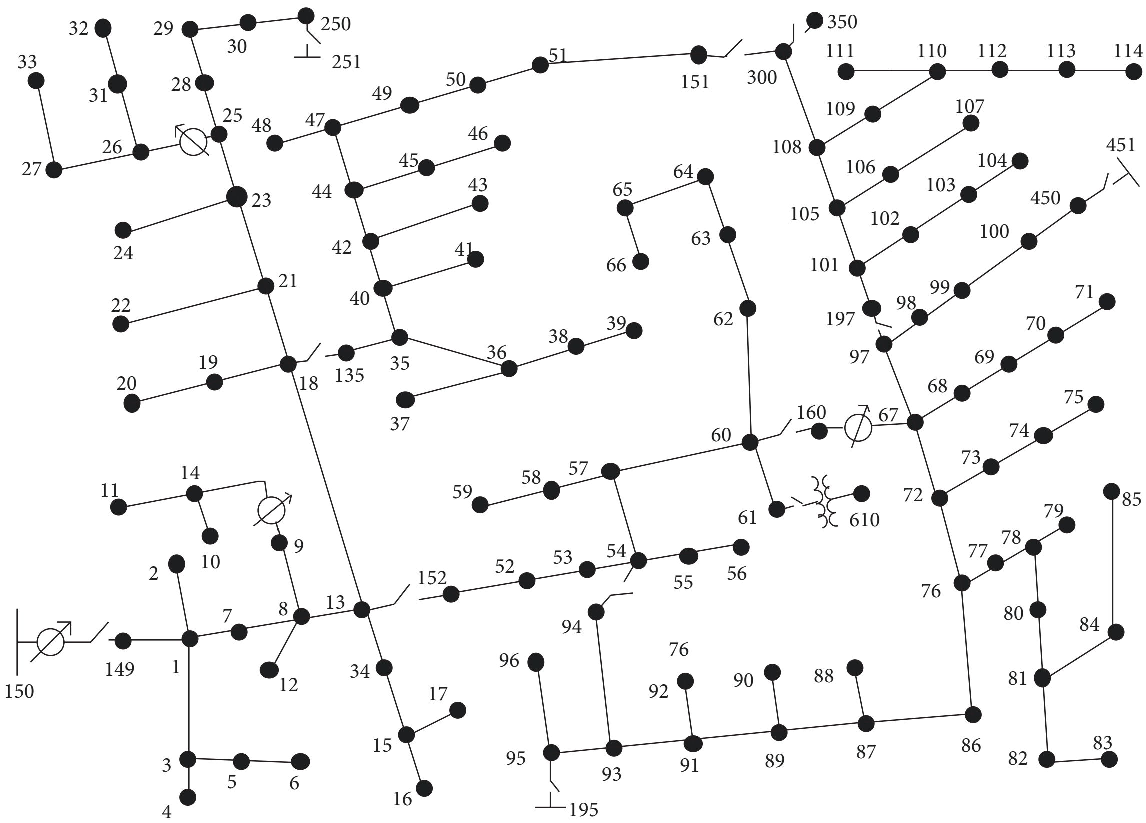

Figure 8: IEEE 123-bus node map.

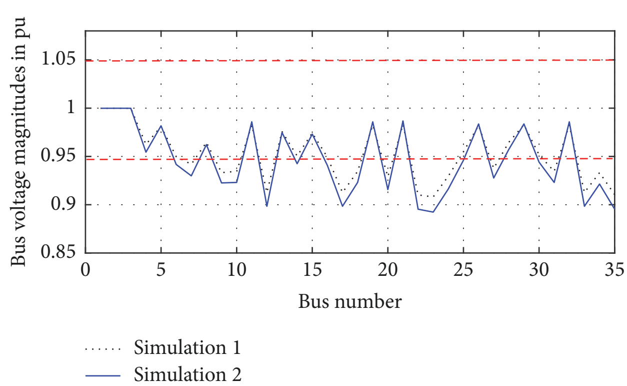

Figure 9: Two different simulation bus voltage magnitudes of IEEE 13-bus test system with no controls.

Table 3: Best results values of IEEE 13-bus test system in simulation I condition.

Load profile condition	Voltage magnitude in pu	Algorithm	No control	Case 1 values	Case 2 values	Case 3 values
Simulation I (minimum load)	Minimum	No control	0.9081	0.9081	0.9081	0.9081
		ICA	0.9081	0.98544	0.98462	0.98684
		PSO	0.9081	0.98544	0.98477	0.97644
		MFO	0.9081	0.98544	0.9846	0.9838
	Maximum	No control	0.99995	0.99995	0.99995	0.99995
		ICA	0.99995	1.0347	1.0209	1.0234
		PSO	0.99995	1.0347	1.022	1.0275
		MFO	0.99995	1.0347	1.0269	1.0227

Table 4: Best results values of IEEE 123-bus test system in simulation II condition.

Load profile condition	Voltage magnitude in pu	Algorithm	No control	Case 1 values	Case 2 values	Case 3 values
Simulation II (maximum load)	Minimum	No control	0.91934	0.91934	0.91934	0.91934
		ICA	0.91934	0.97758	0.98768	0.9685
		PSO	0.91934	0.97758	0.96908	0.9658
		MFO	0.91934	0.97758	0.98338	0.96869
	Maximum	No control	0.99999	0.99999	0.99999	0.99999
		ICA	0.99999	1.035	1.0408	1.0317
		PSO	0.99999	1.035	1.0404	1.0369
		MFO	0.99999	1.035	1.038	1.0334

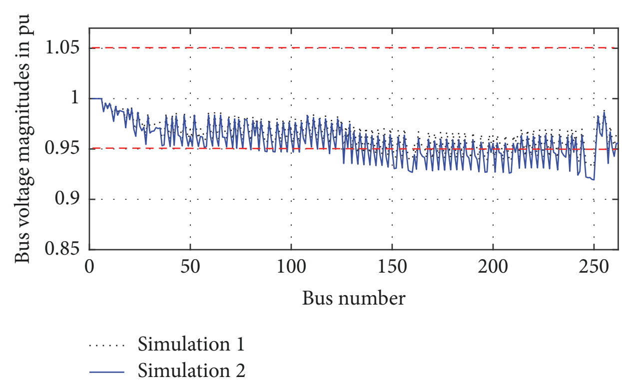

Figure 10: Two different simulation bus voltage magnitudes of IEEE 123-bus test system with no controls.

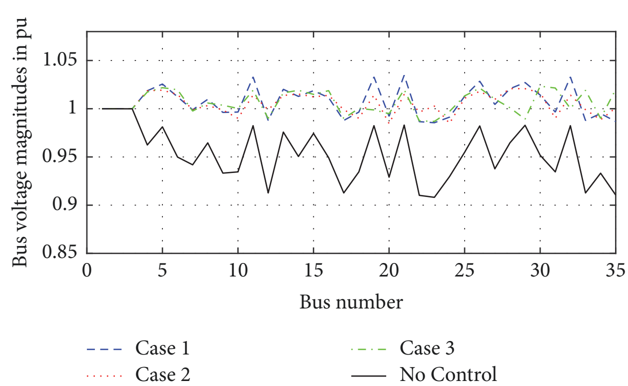

Figure 11: ICA method output of IEEE 13-bus compared to uncontrolled case in simulation I condition.

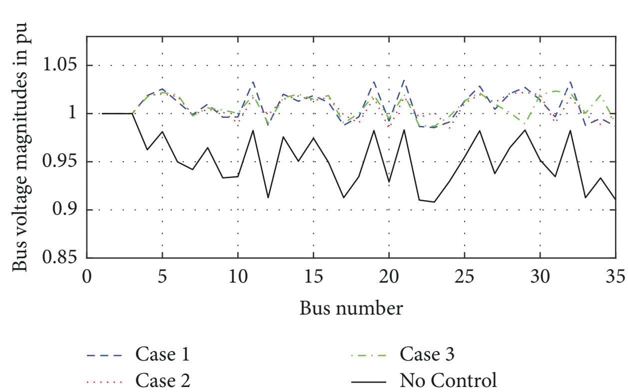

Figure 12: PSO method output of IEEE 13-bus compared to uncontrolled case in simulation I condition.

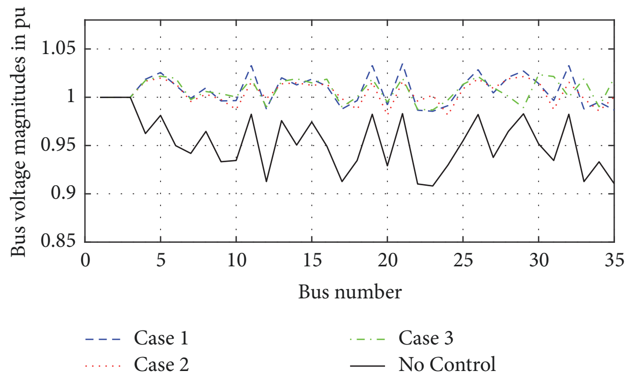

Figure 13: MFO method output of IEEE 13-bus compared to uncontrolled case in simulation I condition.

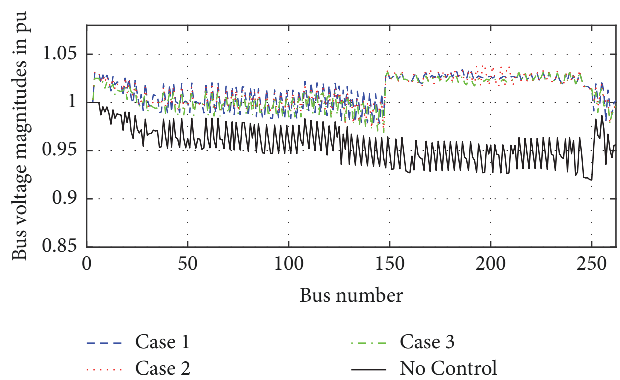

Figure 14: ICA method output of IEEE 123-bus compared to uncontrolled case in simulation II condition.

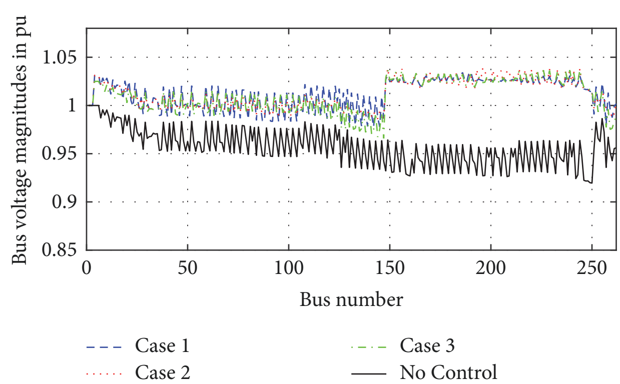

Figure 15: PSO method output of IEEE 123-bus compared to uncontrolled case in simulation II condition.

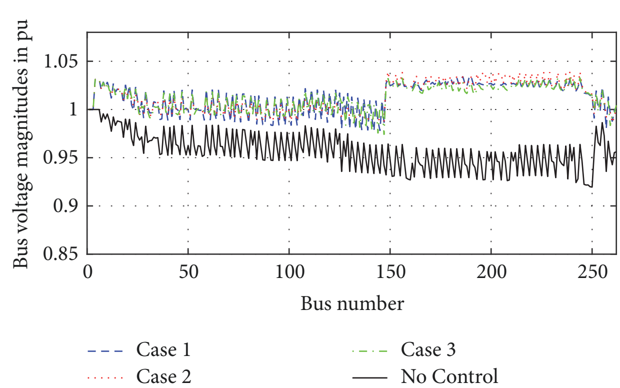

Figure 16: MFO method output of IEEE 123-bus compared to uncontrolled case in simulation II condition.

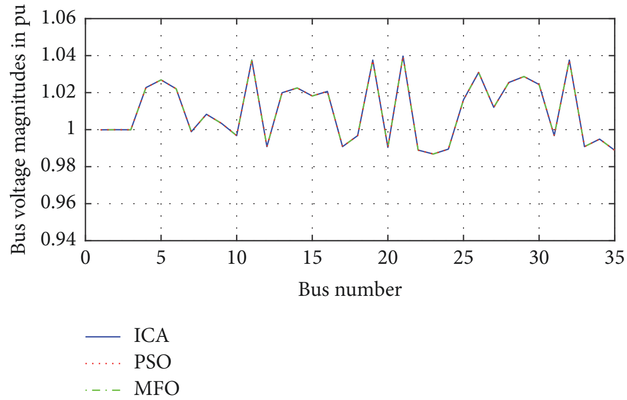

FIGURE 17: Case 1 output of IEEE 13-bus compared to three methods in simulation II condition.

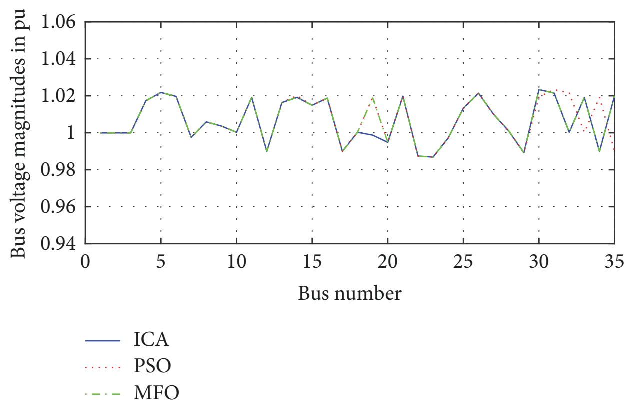

FIGURE 18: Case 3 output of IEEE 13-bus compared to three methods in simulation I condition.

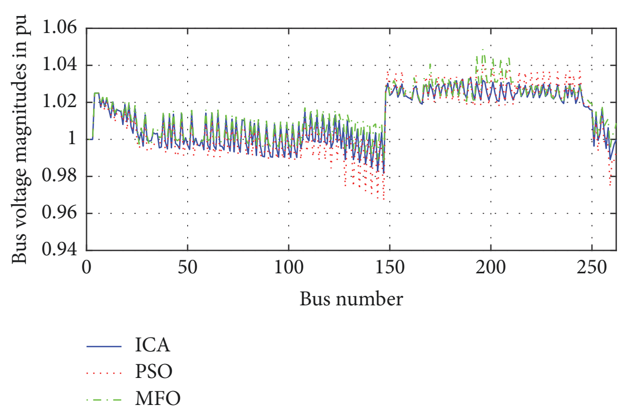

FIGURE 19: Case 2 output of IEEE 123-bus compared to three methods in simulation I condition.

The performance curves in Figures 17–19 demonstrate that improved voltage is achieved in Cases 2 and 3 using ICA as shown in Tables 5 and 6. Meanwhile, as shown in Tables 5 and 6, Case 1 has the same values under all algorithms. The proposed algorithm iteration versus best fitness value in Case 3 of simulation I and simulation II of 13- and 123-bus system is shown in Figures 20 and 21, respectively. Tables 5 and 6 present comparison results, namely, best fitness values, mean voltage magnitudes for best fitness values, and standard deviation voltage magnitudes for best fitness values, in three phases under the different cases and modified heuristic approaches for the IEEE 13- and IEEE 123-bus test systems, respectively.

5. Conclusion

The proposed optimization model is based on three meta-heuristics approaches, namely, particle swarm optimization, imperialist competitive algorithm, and moth flame optimization, for solving the voltage deviation problem. That model

Table 5: Best results values of IEEE 13-bus for 3 phases.

Results type	Load profile condition	Algorithm	No control	Case 1 values	Case 2 values	Case 3 values
Best fitness values; (1) for Case 1, (4) for Case 2, (6) for Case 3	Simulation I (minimum load)	No control	0.10569	0.10569	0.10569	0.10569
		ICA	0.10569	**0.010363**	0.006764	**0.0064852**
		PSO	0.10569	0.010363	0.0060784	0.0068729
		MFO	0.10569	0.010363	**0.0056067**	0.0066113
	Simulation II (maximum load)	No control	0.14316	0.14316	0.14316	0.14316
		ICA	0.14316	**0.013653**	**0.00833**	**0.012759**
		PSO	0.14316	0.013653	0.0086557	0.014014
		MFO	0.14316	0.013653	0.0085749	0.012991
Mean voltage magnitudes for best fitness values	Simulation I (minimum load)	No control	0.95284	0.95284	0.95284	0.95284
		ICA	0.95284	**1.0073**	1.0101	1.0065
		PSO	0.95284	1.0073	1.0063	1.0072
		MFO	0.95284	1.0073	**1.0048**	**1.0046**
	Simulation II (maximum load)	No control	0.94605	0.94605	0.94605	0.94605
		ICA	0.94605	**1.0102**	1.0075	1.0067
		PSO	0.94605	1.0102	**1.006**	1.0079
		MFO	0.94605	1.0102	1.0072	**1.0058**
Standard deviation voltage magnitudes for best fitness values	Simulation I (minimum load)	No control	0.028612	0.028612	0.028612	0.028612
		ICA	0.028612	**0.015797**	**0.0096983**	**0.012119**
		PSO	0.028612	0.015797	0.011767	0.012222
		MFO	0.028612	0.015797	0.011881	0.013154
	Simulation II (maximum load)	No control	0.034842	0.034842	0.034842	0.034842
		ICA	0.034842	**0.017181**	**0.013685**	**0.018152**
		PSO	0.034842	0.017181	0.014732	0.018642
		MFO	0.034842	0.017181	0.014085	0.018644

Table 6: Best results values of IEEE 123-bus for 3 phases.

Results type	Load profile condition	Algorithm	No control	Case 1 values	Case 2 values	Case 3 values
Best fitness values; (1) for Case 1, (4) for Case 2, (6) for Case 3	Simulation I (minimum load)	No control	0.39548	0.39548	0.39548	0.39548
		ICA	0.39548	**0.10046**	**0.087984**	**0.071935**
		PSO	0.39548	0.10046	0.092346	0.088997
		MFO	0.39548	0.10046	0.10902	0.079843
	Simulation II (maximum load)	No control	0.57663	0.57663	0.57663	0.57663
		ICA	0.57663	**0.1038**	**0.093454**	**0.079199**
		PSO	0.57663	0.1038	0.13166	0.10153
		MFO	0.57663	0.1038	0.10887	0.085254
Mean voltage magnitudes for best fitness values	Simulation I (minimum load)	No control	0.96441	0.96441	0.96441	0.96441
		ICA	0.96441	**1.0129**	1.0114	**1.0089**
		PSO	0.96441	1.0129	**1.0108**	1.0113
		MFO	0.96441	1.0129	1.0141	1.0124
	Simulation II (maximum load)	No control	0.95697	0.95697	0.95697	0.95697
		ICA	0.95697	**1.0123**	**1.0116**	**1.009**
		PSO	0.95697	1.0123	1.016	1.0117
		MFO	0.95697	1.0123	1.0122	1.0094
Standard deviation voltage magnitudes for best fitness values	Simulation I (minimum load)	No control	0.015601	0.015601	0.015601	0.015601
		ICA	0.015601	**0.014796**	**0.014398**	0.014012
		PSO	0.015601	0.014796	0.015417	0.014598
		MFO	0.015601	0.014796	0.014815	**0.012326**
	Simulation II (maximum load)	No control	0.018723	0.018723	0.018723	0.018723
		ICA	0.018723	**0.015693**	**0.014916**	**0.014876**
		PSO	0.018723	0.015693	0.015685	0.015844
		MFO	0.018723	0.015693	0.01638	0.015424

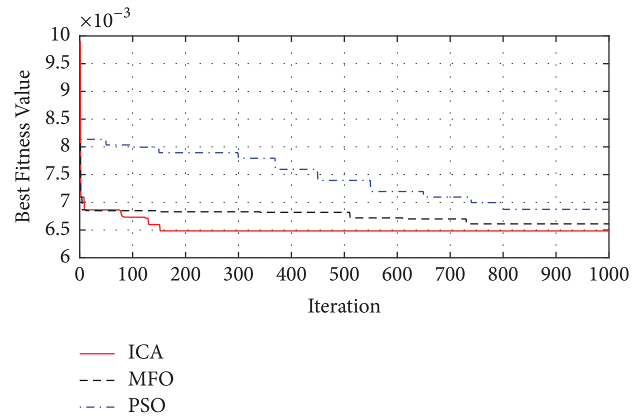

FIGURE 20: : The proposed algorithm iteration versus best fitness value of 13-bus test system in simulation I.

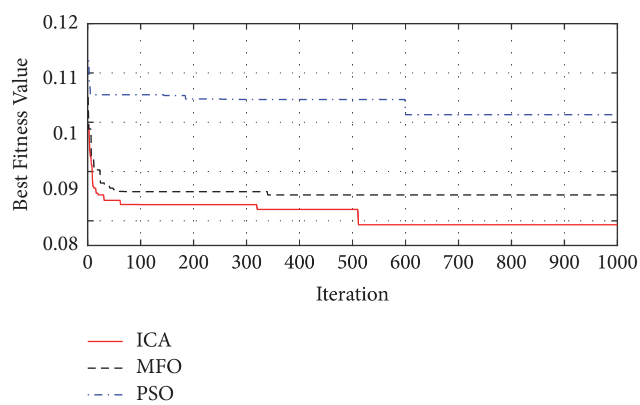

FIGURE 21: The proposed algorithm iteration versus best fitness value of 123-bus test system in simulation II.

uses three different cases: Case 1, changing the tap positions of the regulators; Case 2, changing the capacitor sizes; and Case 3, integrating Cases 1 and 2 and changing the locations of the capacitors. To prove the implementation of the proposed approach, it is applied and demonstrated on the IEEE 13- and IEEE 123-bus test systems. The numerical simulation results show that the voltage deviation problem is solved and the best solution is obtained in Case 3, which considers tap changers for the voltage regulators and the sizes and locations of the capacitors. Moreover, the ICA method provides improved results.

Data Availability

The data used to support the findings of this study are available from the corresponding author upon request.

Conflicts of Interest

The authors declare that there are no conflicts of interest regarding the publication of this paper.

References

[1] L. M. Rios and N. V. Sahinidis, "Derivative-free optimization: a review of algorithms and comparison of software implementations," *Journal of Global Optimization*, vol. 56, no. 3, pp. 1247–1293, 2013.

[2] R. Uluski and M. Mcgranaghan, "Load Models for Voltage Optimization," in *Proceedings of the International Conference on Electricity Distribution*, p. 1312, Frankfurt, Germany, June 2011.

[3] A. Elsheikh, Y. Helmy, Y. Abouelseoud, and A. Elsherif, "Optimal capacitor placement and sizing in radial electric powe r systems," *Alexandria Engineering Journal*, vol. 53, no. 4, pp. 809–816, 2014.

[4] https://www.j-schneider.de/fileadmin/user_upload/j-schneider.de/J._Schneider/pdf/Prospekte/smartactive_e.pdf.

[5] Y. M. Shuaib, M. S. Kalavathi, and C. C. Asir, "Electrical power and energy systems optimal capacitor placement in radial distribution system using gravitational search algorithm," *International Journal of Electrical Power and Energy Systems*, vol. 64, pp. 384–397, 2015.

[6] S. Sultana and P. K. Roy, "Electrical Power and Energy Systems Optimal capacitor placement in radial distribution systems using teaching learning based optimization," *International Journal of Electrical Power and Energy Systems*, vol. 54, pp. 387–398, 2014.

[7] K. Muthukumar and S. Jayalalitha, "Harmony search approach for optimal capacitor placement and sizing in unbalanced distribution systems with harmonics consideration," in *Proceedings of the 1st International Conference on Advances in Engineering, Science and Management, (ICAESM' 12)*, pp. 393–398, IEEE, March 2012.

[8] D. Kaur and J. Sharma, "Electrical Power and Energy Systems Multiperiod shunt capacitor allocation in radial distribution systems," *International Journal of Electrical Power and Energy Systems*, vol. 52, pp. 247–253, 2013.

[9] K. Prakash and M. Sydulu, "Particle swarm optimization based capacitor placement on radial distribution systems," in *Proceedings of the IEEE Power Engineering Society General Meeting*, pp. 1–5, IEEE, Tampa, Fla, USA, June 2007.

[10] D. E. Goldberg and J. H. Holland, "Genetic algorithms and machine learning," *Machine Learning*, vol. 3, no. 2-3, pp. 95–99, 1998.

[11] R. C. Eberhart and J. Kennedy, "A new optimizer using particle swarm theory," in *Proceedings of the 6th International Symposium on Micro Machine and Human Science (MHS '95)*, pp. 39–43, IEEE, Nagoya, Japan, October 1995.

[12] Z. W. Geem, J. H. Kim, and G. V. Loganathan, "A new heuristic optimization algorithm: harmony search," *Simulation*, vol. 76, no. 2, pp. 60–68, 2001.

[13] S. Mirjalili, "Moth-flame optimization algorithm: a novel nature-inspired heuristic paradigm," *Knowledge-Based Systems*, vol. 89, pp. 228–249, 2015.

[14] https://sourceforge.net/p/electricdss/wiki/Home/.

[15] R. C. Dugan, "Open distribution simulations system workshop: Using open dss for smart distribution simulations," in *Proceedings of the EPRI PQ Smart Distribution 2010 Conference and Exhibition*, pp. 14–17, 2010.

[16] E. Atashpaz-Gargari and C. Lucas, "Imperialist competitive algorithm: an algorithm for optimization inspired by imperialistic competition," in *Proceedings of the IEEE Congress on Evolutionary Computation (CEC '07)*, pp. 4661–4667, IEEE, September 2007.

[17] J. Kennedy and R. Eberhart, "Particle swarm optimization," in *Proceedings of the 1995 IEEE International Conference on Neural Networks*, pp. 1942–1948, IEEE Press, Perth, Australia, December 1995.

[18] A. Engelbrecht, *Computational Intelligence: An Introduction*, John Wiley and Sons, 2002.

[19] D. W. van der Merwe and A. P. Engelbrecht, "Data clustering using particle swarm optimization," in *Proceedings of the Congress on Evolutionary Computation (CEC '03)*, vol. 1, pp. 215–220, Canberra, Australia, December 2003.

[20] P. Anbarasan and T. Jayabarathi, "Optimal Reactive Power Dispatch Using Moth-Flame Optimization Algorithm," *International Journal of Applied Engineering Research*, vol. 12, no. 13, pp. 3690–3701, 2017.

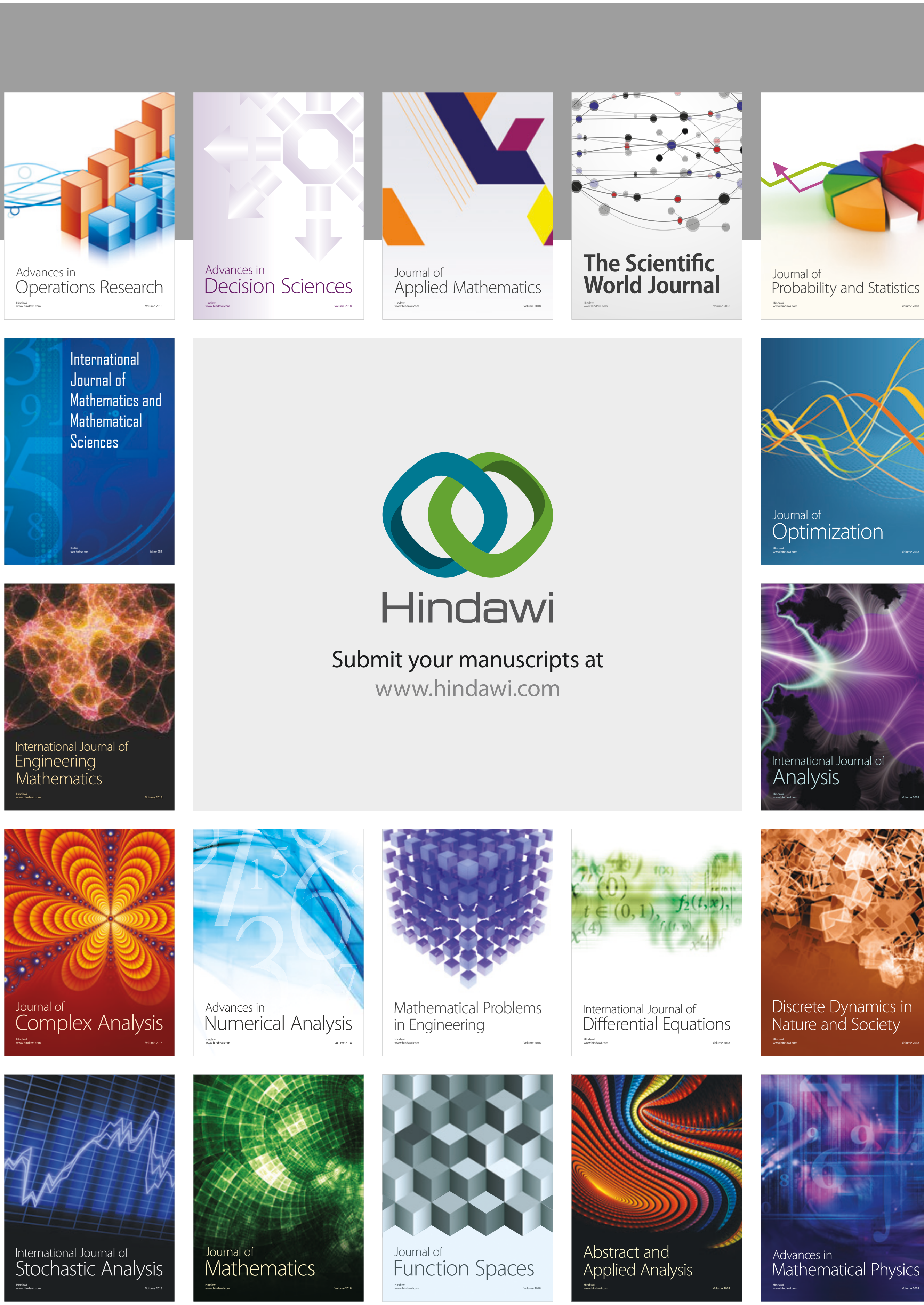
Advances in Operations Research
Advances in Decision Sciences
Journal of Applied Mathematics
The Scientific World Journal
Journal of Probability and Statistics
International Journal of Mathematics and Mathematical Sciences
Hindawi
Submit your manuscripts at
www.hindawi.com
Journal of Optimization
International Journal of Engineering Mathematics
International Journal of Analysis
Journal of Complex Analysis
Advances in Numerical Analysis
Mathematical Problems in Engineering
International Journal of Differential Equations
Discrete Dynamics in Nature and Society
International Journal of Stochastic Analysis
Journal of Mathematics
Journal of Function Spaces
Abstract and Applied Analysis
Advances in Mathematical Physics